Magn Reson Med Sci, Vol. 7, No. 1, pp. 23–29, 2008

MAJOR PAPER

Apparent Diffusion Coefficients of Breast Tumors: Clinical Application

Masamitsu HATAKENAKA[1]*, Hiroyasu SOEDA[1], Hidetake YABUUCHI[1], Yoshio MATSUO[1], Takeshi KAMITANI[1], Yoshinao ODA[2], Masazumi TSUNEYOSHI[2], and Hiroshi HONDA[1]

Departments of [1]Clinical Radiology and [2]Anatomic Pathology,
Graduate School of Medical Sciences, Kyushu University
3–1–1 Maidashi, Higashi-ku, Fukuoka 812–8582, Japan
(Received August 22, 2007; Accepted December 12, 2007)

Purpose: To evaluate the usefulness of apparent diffusion coefficient (ADC) for the differential diagnosis of breast tumors and to determine the relation between ADC and tumor cellularity.

Materials and Methods: One hundred and thirty-six female patients (age range, 17-83 years; average age, 51.7 years) with 140 histologically proven breast tumors underwent diffusion-weighted magnetic resonance (MR) imaging (DWI) using the spin-echo echo-planar technique, and the ADCs of the tumors were calculated using 3 different b values, 0, 500, and 1000 s/mm^2. The diagnoses consisted of fibroadenoma (FA, n = 16), invasive ductal carcinoma, not otherwise specified (IDC, n = 117), medullary carcinoma (ME, n = 3) and mucinous carcinoma (MU, n = 4). Tumor cellularity was calculated from surgical specimens. The ADCs of breast tumors and cellularity were compared between different histological types by analysis of variance and Scheffe's post hoc test. The correlation between tumor cellularity and ADC was analyzed by Pearson correlation test.

Results: Significant differences were observed in ADCs between FA and all types of cancers ($P < 0.05$) and between MU and other types of cancers ($P < 0.01$) and in cellularity between FA and cancers except MU ($P < 0.01$) and between MU and other types of cancers ($P < 0.01$). There was an inverse correlation between ADC and tumor cellularity ($P < 0.01$, $r^2 = 0.451$).

Conclusions: The ADC may potentially help in differentiating benign and malignant breast tumors. Tumor ADC correlates inversely with tumor cellularity.

Keywords: *apparent diffusion coefficient, breast, cellularity, MR imaging, neoplasm*

Introduction

Magnetic resonance (MR) imaging has been a promising modality in characterizing breast lesions and evaluating local extent of disease,[1–4] and its use with gadolinium enhancement has been reported to have high sensitivity in detecting breast cancers.[5–11] Dynamic MR imaging has been shown useful in differentiating malignant from benign breast lesions.[10,11] However, a wide variety of dynamic MR findings have also been reported.[12] MR imaging is not sufficiently accurate in differentiating between malignant and benign breast lesions.

The clinical usefulness of diffusion-weighted MR imaging (DWI) has also been reported in evaluating brain or liver lesions.[13–15] DWI is now considered to be the modality of choice for detecting acute cerebral infarction[16] and differentiating epidermoid cysts from arachnoid cysts.[17] In addition, a correlation between the histologic grade of malignant brain tumors and apparent diffusion coefficient (ADC) has been documented.[18] Recently, several studies have reported that ADC is useful in differentiating malignant from benign breast lesions[19–24] and that there is a relationship between ADC and cellularity.[20] However, neither the relation between ADC and cellularity of the breast tumor nor the usefulness of ADC in the differential diagnosis of breast lesions has been established. Thus, we performed this clinical study to evaluate the usefulness of ADC in characterizing breast tumors and evaluating the relation between ADC and tumor cellularity.

*Corresponding author, Phone: +81-92-642-5695, Fax: +81-92-642-5708, E-mail: mhatake@radiol.med.kyushu-u.ac.jp

Materials and Methods

Participants

A total of 179 consecutive female patients with 183 solid breast tumors underwent MR imaging, including DWI, prior to surgical treatment in our hospital between October 1999 and December 2001. Needle-aspiration biopsy was performed (3 to 10 days) prior to MR imaging in most cases. Nine of these 179 patients were excluded because they underwent chemotherapy prior to MR imaging, and 34 cases were excluded as a result of small lesions and/or poor visualization of the lesions on DWI. Therefore, the study population comprised 136 patients (age range, 17–83 years; average age, 51.7 years) with 140 breast tumors. The diagnoses consisted of fibroadenoma (FA, n = 16); invasive ductal carcinoma, not otherwise specified (IDC, n = 117); medullary carcinoma (ME, n = 3); and mucinous carcinoma (MU, n = 4) according to the recent World Health Organization (WHO) classification. Final diagnoses were established by histopathologic examination of surgically excised specimens in all patients.

MR examination

MR imaging was performed with a 1.5T superconducting magnet (Magnetom Vision and Symphony; Siemens, Erlangen, Germany) and using a CP breast array coil. The patients were laid in a prone position. Following acquisition of routine short inversion time inversion recovery (STIR) axial images (repetition time [TR]/echo time [TE]/inversion time [TI] = 8000/60/150) including both breasts, diffusion-weighted axial images with single-shot spin-echo echo-planar technique (TR/TE = 2000–4000/100–135), fast low angle shot (FLASH) coronal images (TR/TE/flip angle = 20–24/5.6–6/30) with a fat-saturated pulse, and FLASH coronal images with gadolinium-enhancement were obtained sequentially. Subtracted FLASH coronal images (images without gadolinium were subtracted from images with gadolinium) were produced. The slice thickness was 5–6 mm and gaps were 1.5–2 mm for STIR and DW images. For FLASH images, they were 1 mm and 0 mm. Dynamic images were obtained sequentially before and 0, 60, 120, 180, 240, 300, and 360 s after the administration of gadopentetate dimeglumine. In DWI, 90° and 180° radiofrequency pulse series were applied, and 2 motion-probing gradient (MPG) pulses were applied before and after 180° pulse. The data were then collected using an echo-planar readout. Sequential sampling of the k space was used with a bandwidth of 1250 Hz/pixel and 128 lines of data acquired in 0.3 s. Other parameters included: field of view (FOV), 300 to 240 mm; 128 × 128 matrix; and acquisition of one signal. All images were obtained while patients held their breath, and a fat-saturated pulse was used to exclude severe chemical-shift artifacts. DWI was acquired with MPG pulses applied along 3 (x, y, and z axes) directions with 3 different b factors, 0, 500, and 1000 s/mm^2. ADC maps were automatically generated on the operating console using all 7 images (three b factors with 3 MPG pulse directions; when the b factor was 0, only one image was obtained). Circular regions of interest (ROI) of at least 100 mm^2 were designated by one of the authors (HS). Apparent necrotic or cystic components were avoided by referring to other MR images. ADCs were obtained by measuring the intensity of the ROIs on the ADC maps. Tumor diameter was measured on the subtracted FLASH coronal images by one of the authors (HS).

Histologic analysis

Cellularity was analyzed using National Institute of Health (NIH) software, image version 1.63, according to the methods of previous reports.[18,20,25] In consensus, two of the authors (HS and MH) randomly chose 3 FOVs for each tumor from a slide (hematoxylin-eosin stained) without information on diagnoses, and microscopic images (original magnification × 200) were saved for analysis. In consensus, the two carefully determined the density range at which the image would be categorized as cell nuclei, and the extent of the total area of cell nuclei was measured. A wide range was used to measure the extent of the total FOV. Cellularity was defined as the total area of cell nuclei divided by that of the FOV. The mean value was taken as the cellularity for each tumor. Cellularity was analyzed in 123 of a total of 140 tumors. Slides of surgical specimens could not be obtained in the remaining cases.

Statistical analysis

The ADCs of breast tumors and tumor diameters and cellularity were compared between histopathologic diagnoses by analysis of variance and Scheffe's post hoc test to determine if there was any difference between the different histological types. The relation between ADC and cellularity was analyzed by Pearson correlation test to evaluate the effect of cellularity on ADC. $P < 0.05$ was considered significant. The values are expressed as mean ± standard deviation (SD) unless otherwise mentioned. All statistical processing was performed with Stat View version 5.0 software (Japanese version of SAS, Hulinks, Tokyo, Japan) by MH.

Results

Table summarizes the ADCs, cellularity, and tumor diameter of different histological types. Figures 1 and 2 also show the distributions of the ADCs and cellularity. Significant differences in ADC and cellularity ($P<0.01$) were observed between different histological types by analysis of variance. Scheffe's post hoc test showed a significant difference in ADC between fibroadenoma and all types of cancers (FA versus ME, $P<0.01$; FA vs. IDC, $P<0.01$; and ADC of FA is greater than that of ME and IDC; FA vs. MU, $P<0.05$, ADC of FA is smaller than that of MU) and between mucinous carcinoma and other types of cancers ($P<0.01$). There was no significant difference in ADC between invasive ductal carcinoma, not otherwise specified, and medullary carcinoma. A significant difference in cellularity was also observed between FA and ME ($P<0.01$), between FA and IDC ($P<0.01$), and between MU and other types of cancers ($P<0.01$). However, there was no significant difference in cellularity between FA and MU ($P=0.274$) or between IDC and ME. No significant difference in tumor diameter was observed among different histological types. A significant negative correlation between ADC and cellularity was noted ($r^2=0.451$, $P<0.01$) (Fig. 3). Representative MR and microscopic images are demonstrated in Figs. 4–7.

If an arbitrary cut-off value of ADC for differentiating malignant from benign lesions was set at 1.48×10^{-3} mm^2/s, the sensitivity was 83.9%, specificity was 81.3%, and overall accuracy was 83.6%. When 4 cases of mucinous carcinoma were excluded, the sensitivity was 86.7%, specificity was 81.3%, and overall accuracy was 86.0%.

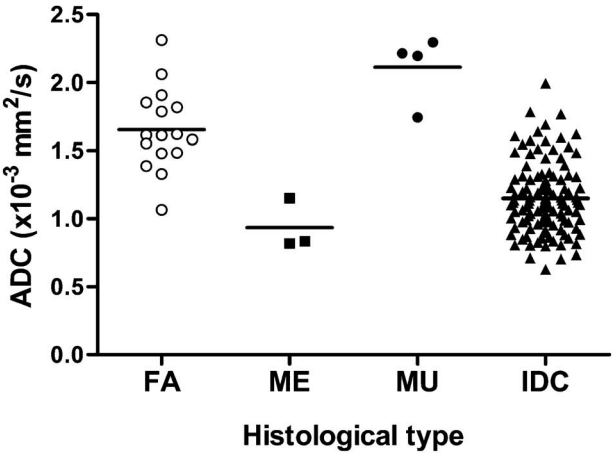

Fig. 1. Distribution of apparent diffusion coefficients. Open circles indicate fibroadenoma; closed squares, medullary carcinoma; closed circles, mucinous carcinoma; and closed triangles, invasive ductal carcinoma, not otherwise specified. Horizontal lines indicate mean values.

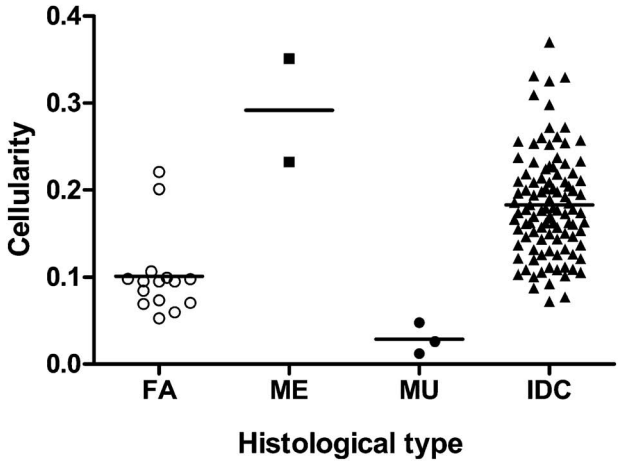

Fig. 2. Distribution of cellularity. Open circles indicate fibroadenoma; closed squares, medullary carcinoma; closed circles, mucinous carcinoma; and closed triangles, invasive ductal carcinoma, not otherwise specified. Horizontal lines indicate mean values.

Table. Characteristics of breast tumors

	Histological type	Numbers of tumors	Diameter (mm)	Apparent diffusion coefficient ($\times10^{-3}$ mm^2/s)	Cellularity
Benign	Fibroadenoma	16(15)*	21.4 ± 7.6	1.66 ± 0.30	0.101 ± 0.047
	Invasive ductal carcinoma, not otherwise specified	117(103)	26.5 ± 12.8	1.15 ± 0.26	0.183 ± 0.060
Malignant	Medullary carcinoma	3(2)	20.7 ± 3.5	0.94 ± 0.15	0.292 ± 0.084
	Mucinous carcinoma	4(3)	20.8 ± 9.6	2.11 ± 0.18	0.028 ± 0.018

* Parentheses enclose numbers of tumors of which cellularity was measured.

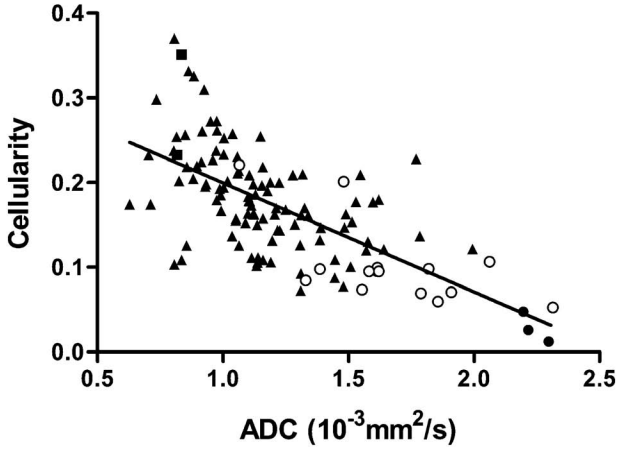

Fig. 3. Correlation of apparent diffusion coefficient (ADC) and cellularity. There is an inverse correlation between ADC and cellularity. The linear regression line is $y = -0.129x + 0.329$. R^2 is 0.451. Open circles indicate fibroadenoma; closed squares, medullary carcinoma; closed circles, mucinous carcinoma; and closed triangles, invasive ductal carcinoma, not otherwise specified.

Discussion

The results of our study indicated that ADC is useful for differentiating fibroadenoma from breast cancer. A significant difference of ADC was observed between FA and all types of cancers. Guo and associates have reported almost the same results and sensitivity of 93%, specificity of 88%, and overall accuracy of 91% when an ADC value of 1.30×10^{-3} mm^2/s or lower is used as a threshold for diagnosing breast cancer.[20] Our results were slightly inferior to theirs, possibly because we did not include breast cysts in our study and because of the difference of disease distribution. Our study consisted of 124 cancers in a total of 140 tumors, and theirs included 31 cancers in a total of 55 lesions. Their study did not include mucinous carcinoma. The slight difference in ADCs (mean ADC of the cancers was 0.97 ± 0.20 and of benign solid lesions, 1.57 ± 0.23) may be partially attributed to the difference in MR sequences employed. We used b values of 0, 500, and 1000 s/mm^2, whereas they used b values of 0 and 1000 s/mm^2 in most cases (42 of a total of 52 cases). Use of a lower b value may slightly increase the ADCs.[20,26] Sinha's group have also reported that malignant breast tumors show lower ADCs than those of benign tumors.[21] These results are also in accordance with ours. The slight difference in ADCs (mean ADC of the cancers was 1.60 ± 0.36 and of benign lesions, 2.01 ± 0.46) may also be due in part to the difference in MR sequences employed. They used lower b values (0–289.7 s/mm^2). Almost the same results have been reported thereafter by the groups of Kuroki, Woodhams, and Rubesova.[22–24] We consider that differential diagnosis based solely on ADC is not sufficiently accurate because of some overlaps in ADC between benign and malignant lesions. Other MR findings, e.g., dynamic pattern, should also be taken into account.

Tumor ADCs and cellularity were well correlated. Our results showed a linear inverse correlation between ADC and cellularity (Fig. 3), and these results agree with previous results.[20] The ADCs are affected by both diffusion and perfusion. The contribution of perfusion to ADC increases when lower b values are employed.[20,26] Buadu and associates have reported that higher microvessel counts are recorded for malignant lesions than for benign.[10] According to their observations, higher ADCs may be expected in cancers compared to benign conditions. However, in our study, the ADCs of cancers other than mucinous carcinoma were less than that of fibroadenoma. The contribution of perfusion to ADC may be considered negligible under our experimental condition; it is also possible that the decrease in ADC by the effect of high cell density may overcome the opposite effect of perfusion in cancers. The diffusion of water in tissue is strongly influenced by fluid viscosity and membrane permeability between intra- and extracellular components, active transport and flow, and directionality of structures that impede or enhance mobility.[27] An order of magnitude difference is reported between the diffusion of slow/intracellular and fast/extracellular water molecules *in vitro*.[28] We consider that the decrease of ADCs observed in cancers other than mucinous carcinomas probably reflects the histologic appearance of dense cellularity causing less extracellular water content and more barrier structures. However, some exceptional cancer cases demonstrated relatively high ADC (Fig. 7). In these cases, a relatively high proliferation of fibrous stroma was observed at histopathologic examination. The increase in extracellular water in the stroma may have contributed to the high ADC.

The ADC of mucinous carcinoma was significantly higher than that of other types of breast cancers and fibroadenoma. On mammography and ultrasonography, imaging features of MU of the breast differ from those of more common breast cancers. Kawashima and colleagues have reported high signal intensity on T_2-weighted images and gradual enhancement pattern on dynamic MR imaging to be specific findings of MU of the breast.[29] We suppose that high ADC may be an additional specific finding for diagnosing MU. Compared to

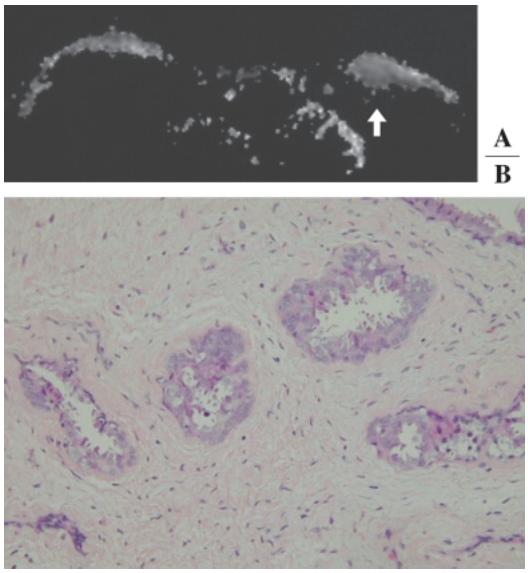

Fig. 4. A representative case of fibroadenoma (44 years). **A)** Axial apparent diffusion coefficient (ADC) map. ADC is 1.615×10^{-3} mm^2/s. Arrow indicates a lesion. **B)** Microscopic image with hematoxylin-eosin stain (original magnification of ×200). Ductal epithelial component is embedded in extensive fibrous stroma. Cellularity is 0.100.

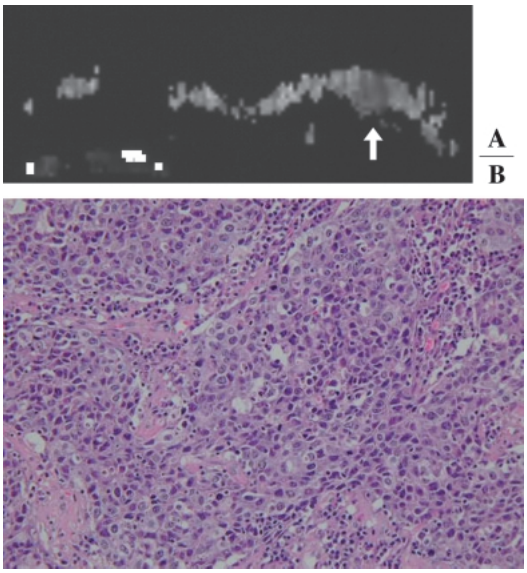

Fig. 6. A representative case of invasive ductal carcinoma, not otherwise specified (36 years). **A)** Axial apparent diffusion coefficient (ADC) map. ADC is 1.158×10^{-3} mm^2/s. Arrow indicates a lesion. **B)** Microscopic image with hematoxylin-eosin stain (original magnification of ×200). Carcinoma cells are proliferating in high density, arranged in sheets. Cellularity is 0.218.

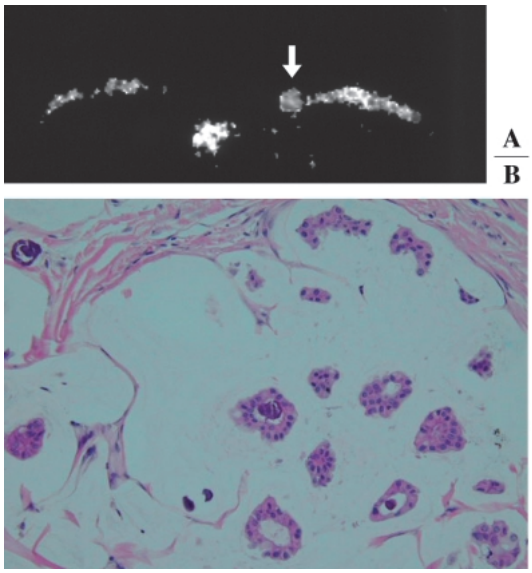

Fig. 5. A representative case of mucinous carcinoma (53 years). **A)** Axial apparent diffusion coefficient (ADC) map. ADC is 2.196×10^{-3} mm^2/s. Arrow indicates a lesion. **B)** Microscopic image with hematoxylin-eosin stain (original magnification of ×200). The clusters of carcinoma cells are floating in abundant mucin. Cellularity is 0.047.

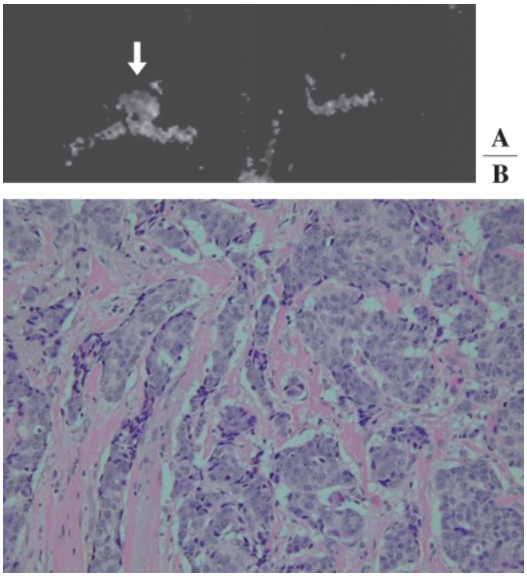

Fig. 7. An exceptional case of invasive ductal carcinoma, not otherwise specified (IDC) (51 years) with relatively high apparent diffusion coefficient (ADC) and low cellularity compared with representative IDCs. **A)** Axial ADC map. ADC is 1.597×10^{-3} mm^2/s. Arrow indicates a lesion. **B)** Microscopic image with hematoxylin-eosin stain (original magnification of ×200). Carcinoma cells proliferate with fibrous stroma. Cellularity is 0.170.

other cancers and fibroadenoma, MU demonstrated lower cell density and higher extracellular water content, which reflected a mucin pool. The very high signal intensity on T_2-weighted images of MU probably reflects high extracellular water content because T_2 relaxation time correlates well with the extent of extracellular water spaces.[25] Although the difference in ADC between FA and MU was significant, the difference in cellularity was not. The water in the mucin pool can probably move more randomly compared to that in the interstitium or cytoplasm of FA. Our study is limited because it includes only 4 cases of MU because MU is rare and comprises only one to 4% of primary breast malignancies.[29] Further study will be needed to clarify details.

Our study has other limitations as well. First, it was impossible to match exactly a histologic specimen with the ROI designated on the DWI; thus, 3 FOVs were randomly chosen for each tumor to minimize the discrepancy between the MR images and the specimens. Second, because small breast lesions are difficult to visualize on DWI, ADC measurement is impossible. We excluded 34 lesions because measurement of ADC of these lesions was impossible on DWI. Those included 4 cases of ductal carcinomas *in situ*. Although the details were not examined in this study, ADC measurement is thought to be possible for tumors greater than or equal to 10 mm in diameter. Third, a small area of necrosis or cystic components not detectable on contrast-enhanced MR images may increase the ADC and lead to misdiagnosis.

In conclusion, the ADC may potentially help differentiate benign and malignant breast tumors, and ADC correlates inversely with cell density.

References

1. Kaiser WA, Zeitler E. MR imaging of the breast: fast imaging sequences with and without Gd-DTPA. Preliminary observations. Radiology 1989; 170:681–686.
2. Harms SE, Flamig DP, Hesley KL, et al. MR imaging of the breast with rotating delivery of excitation off resonance: clinical experience with pathologic correlation. Radiology 1993; 187:493–501.
3. Orel SG, Schnall MD, LiVolsi VA, Troupin RH. Suspicious breast lesions: MR imaging with radiologic-pathologic correlation. Radiology 1994; 190: 485–493.
4. Boetes C, Barentsz JO, Mus RD, et al. MR characterization of suspicious breast lesions with a gadolinium-enhanced TurboFLASH subtraction technique. Radiology 1994; 193:777–781.
5. Orel SG. High-resolution MR imaging for the detection, diagnosis, and staging of breast cancer. Radiographics 1998; 18:903–912.
6. Fischer U, Kopka L, Grabbe E. Breast carcinoma: effect of preoperative contrast-enhanced MR imaging on the therapeutic approach. Radiology 1999; 213:881–888.
7. Orel SG, Schnall MD. MR imaging of the breast for the detection, diagnosis, and staging of breast cancer. Radiology 2001, 220:13–30.
8. Gribbestad IS, Nilsen G, Fjosne H, et al. Contrast-enhanced magnetic resonance imaging of the breast. Acta Oncol 1992; 31:833–842.
9. Gilles R, Guinebretiere JM, Lucidarme O, et al. Nonpalpable breast tumors: diagnosis with contrast-enhanced subtraction dynamic MR imaging. Radiology 1994; 191:625–631.
10. Buadu LD, Murakami J, Murayama S, et al. Breast lesions: correlation of contrast medium enhancement patterns on MR images with histopathologic findings and tumor angiogenesis. Radiology 1996; 200:639–649.
11. Kuhl CK, Mielcareck P, Klaschik S, et al. Dynamic breast MR imaging: are signal intensity time course data useful for differential diagnosis of enhancing lesions? Radiology 1999; 211:101–110.
12. Onishi M, Furukawa A, Takahashi M, Murata K. A wide variety of dynamic contrast-enhanced MR appearances of breast cancer: pathologic correlation study. 2008; 65:286–292. Epub 2007 Aug 1.
13. Noguchi K, Watanabe N, Nagayoshi T, et al. Role of diffusion-weighted echo-planar MRI in distinguishing between brain abscess and tumor: a preliminary report. Neuroradiology 1999; 41:171–174.
14. Yamada I, Aung W, Himeno Y, Nakagawa T, Shibuya H. Diffusion coefficients in abdominal organs and hepatic lesions: evaluation with intravoxel incoherent motion echo-planar MR imaging. Radiology 1999; 210:617–623.
15. Namimoto T, Yamashita Y, Sumi S, Tang Y, Takahashi M. Focal liver masses: characterization with diffusion-weighted echo-planar MR imaging. Radiology 1997; 204:739–744.
16. Burdette JH, Ricci PE, Petitti N, Elster AD. Cerebral infarction: time course of signal changes on diffusion-weighted MR images. AJR Am J Roentgenol 1998; 171:791–795.
17. Tsuruda JS, Chew WM, Moseley ME, Norman D. Diffusion-weighted MR imaging of the brain: value of differentiating between extraaxial cysts and epidermoid tumors. AJNR Am J Neuroradiol 1990; 11:925–931.
18. Sugahara T, Korogi Y, Kochi M, et al. Usefulness of diffusion-weighted MRI with echo-planar technique in the evaluation of cellularity in gliomas. J Magn Reson Imaging 1999; 9:53–60.
19. Kinoshita T, Yashiro N, Ihara N, Funatu H, Fukuma E, Narita M. Diffusion-weighted half-Fourier single-shot turbo spin echo imaging in breast tumors: differentiation of invasive ductal carcinoma

from fibroadenoma. J Comput Assist Tomogr 2002; 26:1042–1046.
20. Guo Y, Cai YQ, Cai ZL, et al. Differentiation of clinically benign and malignant breast lesions using diffusion-weighted imaging. J Magn Reson Imaging 2002, 16:172–178.
21. Sinha S, Lucas-Quesada FA, Sinha U, DeBruhl N, Bassett LW. *In vivo* diffusion-weighted MRI of the breast: potential for lesion characterization. J Magn Reson Imaging 2002; 15:693–704.
22. Kuroki Y, Nasu K, Kuroki S, et al. Diffusion-weighted imaging of breast cancer with the sensitivity encoding technique: analysis of the apparent diffusion coefficient value. Magn Reson Med Sci 2004; 3:79–85.
23. Woodhams R, Matsunaga K, Kan S, et al. ADC mapping of benign and malignant breast tumors. Magn Reson Med Sci 2005; 4:35–42.
24. Rubesova E, Grell AS, De Maertelaer V, Metens T, Chao SL, Lemort M. Quantitative diffusion imaging in breast cancer: a clinical prospective study. J Magn Reson Imaging 2006; 24:319–324.
25. Hatakenaka M, Ueda M, Ishigami K, Otsuka M, Masuda K. Effects of aging on muscle T_2 relaxation time: difference between fast- and slow-twitch muscles. Invest Radiol 2001; 36:692–698.
26. Le Bihan D, Breton E, Lallemand D, Aubin ML, Vignaud J, Laval-Jeantet M. Separation of diffusion and perfusion in intravoxel incoherent motion MR imaging. Radiology 1988; 168:497–505.
27. Sinha S, Sinha U. Functional magnetic resonance of human breast tumors diffusion and perfusion imaging. Ann N Y Acad Sci 2002; 980:95–115.
28. Pilatus U, Shim H, Artemov D, Davis D, van Zijl PC, Glickson JD. Intracellular volume and apparent diffusion constants of perfused cancer cell cultures, as measured by NMR. Magn Reson Med 1997; 37:825–832.
29. Kawashima M, Tamaki Y, Nonaka T, et al. MR imaging of mucinous carcinoma of the breast. AJR Am J Roentgenol 2002; 179:179–183.